

- of the Tenth International TOVS Study Conference, Boulder, Colorado, 1999.
21. Singh, D., Bhatia, R. C. and Srivastav, S. K., Satellite analysis of tropical cyclone using NOAA-16 measurements over Indian regions. *Mausam*, 2004, **55**, 149–154.
 22. Singh, D., Bhatia, R. C. and Prasad, S., A neural network based algorithm for the retrieval of TPW from AMSU measurements. In Fourteenth International TOVS/ATOVS Workshop, Beijing, China, 25–31 May 2005.
 23. Singh, D. and Bhatia, R. C., Study of temperature and moisture profiles retrieved from microwave and hyperspectral infrared sounder data over Indian regions. *Indian J. Radio Space Phys.*, 2006, **35**, 286–292.
 24. Sandeep, S., Chandrasekar, A. and Singh, D., The impact of assimilation of AMSU data on the prediction of a tropical cyclone over India using a mesoscale model. *Int. J. Remote Sensing*, 2006, **27**, 4621–4653.
 25. Lavanant, L., Brunel, P., Rochard, G., Labrot, T. and Pochic, D., Current status for the ICI retrieval scheme. Technical Proceedings of the Ninth International TOVS Study Conference, 1997.
 26. Lavanant, L., Brunel, P., Rochard, G. and Labrot, T., NOAA15 soundings profiles retrieved with the ICI scheme. Technical Proceedings of the Tenth International TOVS Study Conference, 1999.
 27. Ere, J. R., A fast radiative transfer model for satellite soundings system. ECMWF Technical Memorandum No. 176, 1991.
 28. Sanders, R., Matricardi, M. and Brunel, P., An improved fast radiative transfer model for assimilation of radiance observations. *Q. J. R. Meteorol. Soc.*, 1998, **102**, 1407–1425.
 29. Li, J., Wolf, W. W., Menzel, W. P., Zhang, W. J., Huang, H. L. and Achtor, T. H., Global sounding of the atmosphere from ATOVS measurement: The algorithm and validation. *J. Appl. Meteorol.*, 2000, **39**, 1248–1268.

ACKNOWLEDGEMENTS. Thanks are due to EUMETSAT for providing the AAPP4.0 and ICI3.0 software. I also thank Dr Lydie Lavanant, Météo-France for help in the installation of the ICI software and for useful suggestions. I also thank IMD and DAAC/NASA for providing the ATOVS and AIRS data respectively.

Received 12 December 2006; revised accepted 29 August 2007

Finite difference modelling of scattered hydrates and its implications in gas-hydrate exploration

P. Dewangan*, T. Ramprasad and M. V. Ramana

National Institute of Oceanography, Goa 403 004, India

Gas-hydrates have drawn considerable attention in the scientific community due to their importance as an alternative energy source. One of the best tools for hydrate exploration is conventional 2D reflection seismics, which records the base of the hydrate stability zone manifested in the form of a bottom-simulating reflector (BSR). The conventional seismic data depict BSR as a continuous layer and this can be misleading in the mapping and prediction of reserves, while high-

frequency seismic and drilling data collected worldwide have shown gas-hydrates to be scattered deposits. We have investigated the seismic response of scattered hydrates with varying frequencies and shown that BSR amplitudes in 2D seismics can be misleading if the size of the Fresnel zone is larger than the distance between the scatterers.

Keywords: Bottom-simulating reflector, exploration, gas-hydrates, 2D seismics, scatterers.

RECENTLY, high-frequency seismic data were collected to understand the formation and distribution of hydrates in the Cascadia accretionary margin off Vancouver Island¹, Blake Ridge² and Lake Baikal³. Such studies can be broadly divided into three categories: air-gun/sleeve gun (4–300 Hz), sparker sources (400–1000 Hz) and Deep-Towed Acoustics/Geophysics System (DTAGS; 250–650 Hz). Analysis of these datasets led to an important conclusion that the gas-hydrates are scattered with large lateral variations rather than occurring in a continuous form. This inference is reasonable as the hydrate distribution is governed by the availability and movement of hydrocarbon gases rather than by a depositional process. The bottom-simulating reflector (BSR) in high-frequency data is characterized by a series of closely spaced, dipping, enhanced reflections with varying lateral extent^{3,4}, in contrast to laterally continuous reflection as observed in low-frequency data. This observation can be explained by the size of the Fresnel zone⁵, which is defined as the lateral distance over which the reflection signal is averaged. The size of the Fresnel zone determines the minimum size feature that can be resolved from the seismic data (Figure 1); smaller Fresnel zone results in better resolution. The radius of the Fresnel zone⁵ (R) for zero-offset, unmigrated section depends on the medium velocity (V), the two-way travel time of the reflection (T), and the dominant wavelength of the seismic wavelet (λ) as:

$$R = \frac{1}{2} \sqrt{V \lambda T}. \quad (1)$$

High-frequency data having smaller Fresnel zone show discontinuous BSR, whereas low-frequency data having larger Fresnel zone show continuous BSR from the scattered hydrates⁶. Moreover, BSRs appear weak in high-frequency seismic data in contrast to strong reflection observed in the low-frequency seismics. This frequency dependence of BSR amplitudes is due to the gradational velocity structure at the base of the hydrate stability zone (BHSZ)¹. As a result, the velocity difference between the hydrate and free gas will be represented as a step change for low-frequency data in contrast to a gradual change in high-frequency data. This gradual change results in smaller impedance contrast that weakens the amplitude of the BSR. Reflection from the top of the hydrate-bearing zone and the base of the free gas layer is generally not resolved

*For correspondence. (e-mail: pdewangan@nio.org)

in conventional seismics supporting the hypothesis of gradual velocity gradients⁷.

In order to understand the seismic response of scattered hydrates, we simulated 2D seismic data using traditional explicit second order acoustic finite difference modelling⁸. We used the Seismic Unix code (sufdmod2) for all numerical simulations⁹. As a rule, the number of grid points should be ten or more per wavelength to avoid grid dispersion effect¹⁰. The time step was calculated from grid spacing and maximum velocity based on the stability criteria of finite difference algorithm⁸. Since the computational domain has to be truncated to keep the reasonable resource requirement, the finite difference algorithms have difficulties in dealing with open-region problems. We eliminated the edge reflections using perfectly matched layers (PML), as discussed by Berenger¹¹. This method provides a reflection-less interface between the region of interest and the lossy PML at all incident angles. As the wave propagates through the PML, its amplitude is significantly attenuated.

The dimension of the model was arbitrarily chosen with a variable grid size depending on the stability analysis. The thickness of the hydrate stability zone and water column was assumed to be 200 and 1000 m respectively. The *P*-wave velocity in the water column was set to 1480 m/s. In order to simulate the effect of compaction of marine sediments, the background velocity was increased linearly with depth assuming a velocity gradient of 300 m/s per km. The discontinuous hydrate layers were modelled as sporadic distribution, preferentially deposited along the nodal points at the BHSZ. These nodal points may be assumed as the locations of micro-cracks, acting as conduits for the movement of hydrocarbon gases. The horizontal locations of nodal points were extracted from a uniform distribution of gaps between the scatterers to cover a wide range. The horizontal distribution of hydrates was modelled using two-sided Gaussian membership function of limited horizontal extent (~15 m) centred at

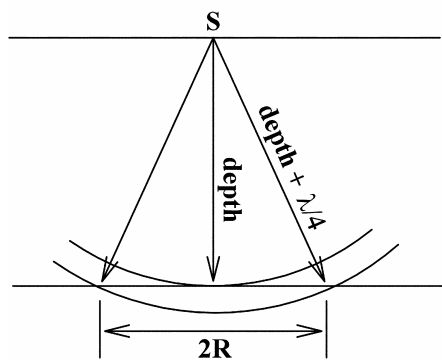


Figure 1. Diagram illustrating Fresnel zone ($2R$), lateral distance over which the reflection signal is averaged. The dominant wavelength of the seismic wave is represented by λ and R is the radius of the Fresnel zone.

the nodal point. The study of known hydrate deposits shows a gradational velocity profile¹⁻³. Therefore, vertical distribution of the hydrates was modelled using one-sided Gaussian membership function with maximum concentration at BHSZ and reducing to zero at a distance of 15 m from the BHSZ. In a similar fashion, the free gas below the BHSZ was modelled. The Gaussian function produces the necessary smooth velocity gradients for the hydrates as well as the gas layer. Though it is not simple to calculate the seismic velocity from hydrate saturation; we made an attempt assuming a linear relationship to perturb the background velocity model based on hydrate saturation. The sea bottom reflection coefficient is primarily due to the density contrast between the water column and the sediments. Therefore, the density of the water column was set to be 1 g/cc and the sediment density assumed to be 1.5 g/cc. In the regions of known hydrate deposits, BSR usually crosscuts the existing geological strata. To simulate this feature, a few anticlinal geological layers with different density were incorporated in the density model. In the density model, it was assumed that the anticlinal geological layers do not perturb the pressure and temperature condition, so that the BSR remains parallel to the seafloor. The velocity and density models used in simulating scattered hydrates are shown in Figure 2.

The zero-offset seismic response for the modelled velocity and density fields was obtained using finite difference modelling code of Seismic Unix⁹. To minimize the edge reflection, sufficiently thick absorbing PML were used and the response calculated for the central portion of the grid. Reflection from the water bottom was due to the sharp density contrast between the water column and the seabed whereas the BSR was primarily due to velocity contrast between the gas-hydrates and free gas. Enlarged zero-offset sections are illustrated in Figure 3 for various widths of the Fresnel zone. The velocity model shown in Figure 3a indicates the positions of the hydrate deposit (scatterers). Figure 3b-d represents the surface-towed source-receiver configuration, where the dominant frequency of the seismic wavelet was varied from 10 to 80 Hz. Figure 3e shows the deep-towed source-receiver configuration, where the source and receiver were located 50 m above the ocean-bottom. The calculated size of the Fresnel radius⁵ is illustrated as solid line in all the plots of Figure 3. Due to smooth velocity gradient, the BSR becomes weaker as the frequencies increase¹, but for comparison all the plots were normalized by the maximum amplitude of the BSR. If the width of the Fresnel zone is larger than the gap between the scatterers (Figure 3b and c), the locations predicted from BSR amplitudes do not agree with the actual locations of the hydrate deposits. For example, high-amplitude BSR reflection from low-frequency data suggests spurious hydrates around 600 m along the profile. Likewise, weak/absence of BSR amplitude around 750 m fails to identify the hydrate at that location. This observation can also be explained by

Kirchoff theory, which states that each scatterer acts as a secondary source and the BSR amplitude is an average of all the energies coming from individual scatterers¹². However, the scatterers which lie within the first Fresnel zone interfere constructively. Therefore, the BSR amplitude in a zero-offset section represents all the scatterers lying within the first Fresnel zone. For high-frequency deep-tow data (Figure 3 *e*), the width of the Fresnel zone was small, resulting in accurate prediction of hydrate locations. The spatial resolution of the seismic data can be

improved by minimizing the width of the Fresnel zone, by lowering the receiver array (geophones/hydrophones) through the earth until the source and receiver coincide with the reflector. This can be achieved using a process known as seismic migration.

After migration¹³ the Fresnel zone will shrink to a small circle of radius of approximate dimension $\lambda/4$, where λ represents the dominant wavelength. The migrated zero-offset sections for the scattered hydrates are shown in Figure 4. The data appear under-migrated, because they

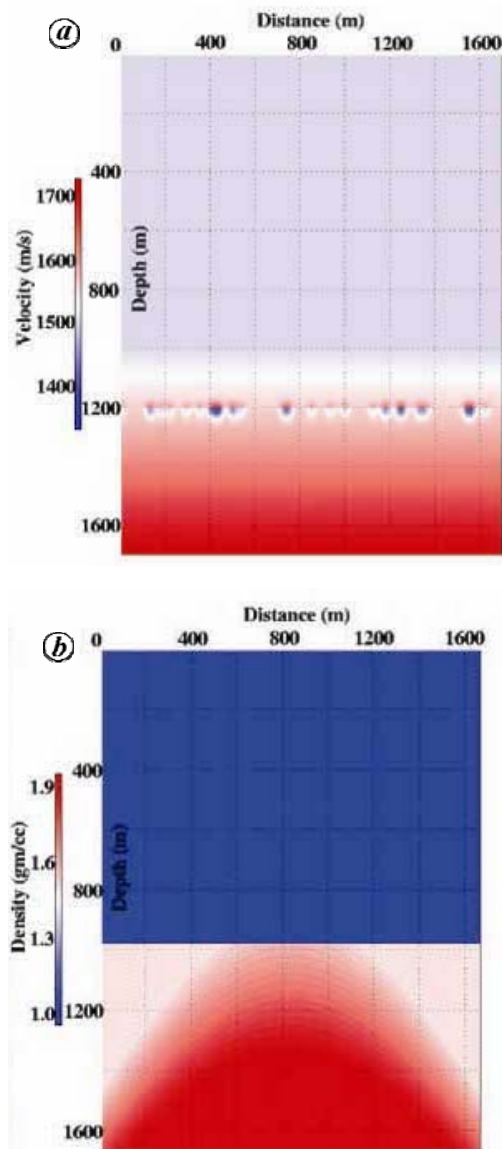


Figure 2. Velocity and density models used in finite difference. Grid dimension was arbitrarily chosen as 1700×1700 m. Thickness of hydrate stability zone and water column was assumed to be 200 and 1000 m respectively. *a*, Velocity model pertaining to scattered hydrates. *b*, Density model representing some anticlinal geological layers.

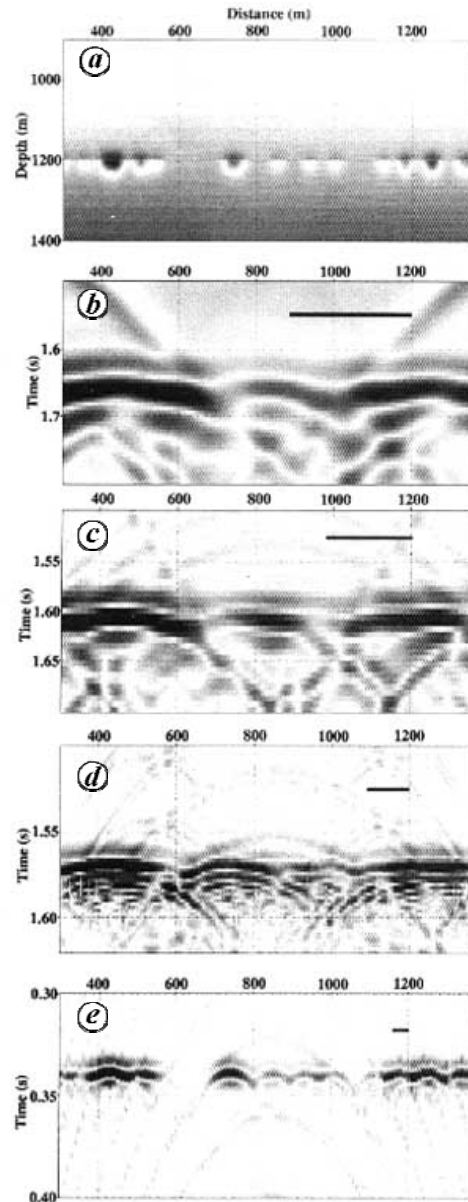


Figure 3. Zero-offset, unmigrated seismic response of the scattered hydrate deposits. *a*, Reference velocity model. Dominant frequencies for (b)–(e) are 10, 20, 80, and 80 Hz respectively. *b*–*d*, Surface-towed configuration. *e*, Deep-towed settings. Thick solid line represents radius of the Fresnel zone.

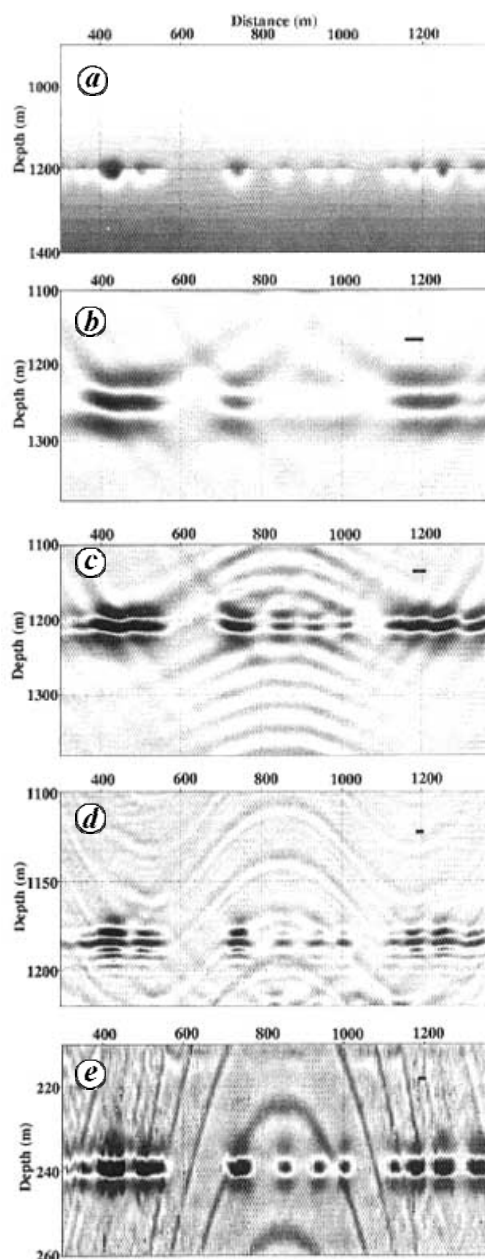


Figure 4. Same as Figure 3, but with all the seismic data migrated using background velocity field.

are migrated with background velocity field instead of true velocity model. In general, the hydrate locations predicted after migration were relatively better than those predicted from unmigrated data. However, if either the data or migration algorithm is two-dimensional, then the Fresnel zone will only shrink in the shooting direction and will still extend its full width in the perpendicular direction. Therefore, the BSR amplitudes in 2D seismics can be misleading if the width of the Fresnel zone is larger

than the distance between the scatterers. The conventional 2D seismic investigations for mapping gas-hydrates in a large area may be advantageous. However, for accurate mapping of the spatial extent of gas-hydrates deposits, seismic data having high vertical and horizontal resolution are required. This can be achieved using higher frequency energy sources or deep-tow source receiver configuration. The migrated 3D seismic data can also be used to map hydrate deposits, as the data have high spatial resolution.

1. Chapman, N. R., Gettrust, J. F., Walia, R., Hannay, D., Spence, G. D., Wood, T. W. and Hyndman, R. D., High-resolution, deep-towed, multichannel seismic survey of deep-sea gas hydrates off western Canada. *Geophysics*, 2002, **67**, 1038–1047.
2. Rowe, M. M. and Gettrust, J. F., Fine structure of methane hydrate-bearing sediments on the Blake Outer Ridge as determined from deep-tow multichannel seismic data. *J. Geophys. Res.*, 1993, **98**, 463–474.
3. Vanneste, M., Batist, M. D., Golmshtok, A., Kremlev, A. and Versteeg, W., Multi-frequency seismic study of gas hydrate-bearing sediments in Lake Baikal, Siberia. *Mar. Geol.*, 2001, **172**, 1–21.
4. Wood, W. T., Gettrust, J. F., Chapman, N. R., Spence, G. D. and Hyndman, R. D., Decreased stability of methane hydrates in marine sediments owing to phase-boundary roughness. *Nature*, 2002, **420**, 656–660.
5. Sheriff, R. E., Nomogram for Fresnel-zone calculation. *Geophysics*, 1980, **45**, 968–972.
6. Spence, G. D., Minshull, T. A. and Fink, C. R., Seismic studies of methane hydrates offshore Vancouver Island. Proceedings of the Ocean Drilling Program, 1995, vol. 146, pp. 163–174.
7. Hyndman, R. D. and Spence, G. D., A seismic study of methane hydrate marine bottom-simulating reflectors. *J. Geophys. Res.*, 1992, **97**, 6683–6698.
8. Kelly, K. R., Ward, R. W., Treitel, S. and Alford, R. M., Synthetic seismograms: A finite-difference approach. *Geophysics*, 1976, **41**, 2–27.
9. Stockwell Jr, J. W., Free software in education: A case study of CWP/SU: Seismic Unix. *Leading Edge*, 1997, **16**, 1045–1050.
10. Alford, R. M., Kelly, K. R. and Boore, D. M., Accuracy of finite-difference modeling of the acoustic wave equation. *Geophysics*, 1974, **39**, 834–842.
11. Berenger, J. P., A perfectly matched layer for the absorption of electromagnetic waves. *J. Comput. Phys.*, 1996, **114**, 185–200.
12. Hilterman, F. J., Interpretative lessons from three-dimensional modeling. *Geophysics*, 1982, **47**, 784–808.
13. Vermeer, G. J. O., Factors affecting spatial resolution. *Geophysics*, 1999, **64**, 942–953.

ACKNOWLEDGEMENT. We thank the Director, NIO, Goa for permission to publish this article. This is NIO contribution no. 4287.

Received 18 December 2006; revised accepted 3 September 2007